GSA Data Repository 2015363

A sub-crustal piercing point for North Atlantic reconstructions and tectonic implications

Christian Schiffer, Randell A. Stephenson, Kenni D. Petersen, Søren B. Nielsen, Bo H. Jacobsen, Niels Balling, and David I.M. Macdonald

Table DR1: Station list, including station names, coordinates, elevation, instrument type and number of processed events.

Station name	Latitude [°]	Longitude [°]	Elevation [m]	Instrument	Number of events
Central Fjord array					
01A	**72.930**	**-28.830**	**1524**	**Güralp 3TD**	**40**
02A	**72.755**	**-28.082**	**1047**	**Güralp 3EX**	**43**
03A	**72.911**	**-27.586**	**44**	**Güralp 3TD/3TD***	**7**
04A	**72.844**	**-27.115**	**1110**	**Güralp 3TD**	**44**
05A	**72.798**	**-26.213**	**1115**	**Güralp 3TD/3EX***	**27**
06A	**72.880**	**-25.118**	**36**	**Güralp 3TD**	**31**
07A	**73.030**	**-24.351**	**90**	**Güralp 3TD**	**49**
08A	**73.065**	**-23.057**	**55**	**Güralp 3TD**	**17**
09A	**73.104**	**-21.437**	**127**	**Güralp 3TD**	**62**
10A	**73.503**	**-20.805**	**193**	**Güralp 3TD**	**42**
11A	**73.274**	**-26.452**	**1260**	**Güralp 3EX**	**34**
Northern Scotland					
STOR	**58.24**	**-5.35**	**-**	**-**	**25**
INCH	**58.15**	**-4.97**	**-**	**-**	**30**
ALTA	**58.29**	**-4.41**	**-**	**-**	**13**
BASS	**58.48**	**-4.20**	**-**	**-**	**25**
BIGH	**58.49**	**-3.91**	**-**	**-**	**30**
ORE	**58.55**	**-3.76**	**-**	**-**	**34**
HOYT	**58.83**	**-3.24**	**-**	**-**	**14**

* This instrument got exchanged during the maintenance in summer 2010.

Table DR2: List of processed events, showing date, magnitude, epicentral distance, backazimuth and for which station. Data from National Earthquake Information Center Earthquake Catalog

				Used at stations										
Date (date/month/ year)	**Mag**	**Lat (°)**	**Lon (°)**	**01A**	**02A**	**03A**	**04A**	**05A**	**06A**	**07A**	**08A**	**09A**	**10A**	**11A**
09/08/2009	7.1	33.17	137.94			X			X					
10/08/2009	7.5	14.10	92.90		X	X			X	X	X	X	X	
12/08/2009	6.6	32.82	140.40		X	X	X		X		X	X		
16/08/2009	6.7	-1.48	99.49						X	X				
17/08/2009	6.7	23.50	123.50		X	X	X		X	X	X	X	X	
03/09/2009	6.2	31.14	130.01		X		X		X		X	X		
07/09/2009	6.0	42.66	43.44									X	X	
10/09/2009	6.0	48.32	154.19		X		X				X		X	
12/09/2009	6.0	10.71	-67.93				X							
21/09/2009	6.1	27.33	91.44							X				
24/09/2009	5.0	46.64	90.20			X	X						X	
30/09/2009	7.6	-0.72	99.87		X	X				X	X	X	X	
03/10/2009	6.1	23.63	121.45									X	X	
13/10/2009	6.4	52.60	-167.12										X	
22/10/2009	6.2	31.14	130.01		X				X	X		X	X	
30/10/2009	6.8	29.22	129.78				X		X					
17/11/2009	6.6	52.12	-131.40		X	X	X		X	X	X	X	X	
17/12/2009	5.6	36.46	-9.90								X			
19/12/2009	6.4	23.80	121.61				X						X	
26/02/2010	7.0	25.93	128.43		X		X					X	X	
13/03/2010	5.2	52.79	160.36										X	
14/03/2010	6.5	37.75	141.59	X	X		X		X	X		X	X	
30/03/2010	6.7	13.67	92.83		X		X		X	X		X	X	
04/04/2010	7.2	32.30	-115.28	X	X		X		X			X	X	
06/04/2010	7.8	2.38	97.05	X	X		X		X	X		X	X	
13/04/2010	6.9	33.17	96.55		X		X		X	X		X	X	
16/04/2010	5.7	54.49	-161.04	X			X						X	
26/04/2010	6.5	22.18	123.63						X			X		
30/04/2010	6.5	60.47	-177.88	X	X		X		X	X		X	X	
02/05/2010	5.4	57.36	162.20	X									X	
03/05/2010	6.1	29.64	140.97	X	X		X			X		X	X	
03/05/2010	5.5	52.61	-163.69	X			X			X		X	X	
09/05/2010	7.2	3.75	96.02	X	X				X	X		X	X	
16/05/2010	5.8	18.40	-67.07				X							
17/05/2010	5.3	46.29	152.02						X					
23/05/2010	5.0	35.96	4.14							X				
24/05/2010	6.5	-8.09	-71.56	X	X		X		X	X		X	X	
25/05/2010	6.3	35.34	-35.92	X	X		X		X	X				
26/05/2010	6.5	25.77	129.94	X	X		X		X	X		X	X	
31/05/2010	6.5	11.13	93.47										X	
01/06/2010	6.0	9.33	-84.21				X			X				
05/06/2010	5.5	43.43	146.77		X		X							
12/06/2010	7.5	7.88	91.94		X				X	X		X	X	
13/06/2010	5.9	37.37	141.63	X	X		X					X		
18/06/2010	6.2	44.45	148.69	X			X			X		X	X	
30/06/2010	6.3	16.40	-97.78	X			X		X	X		X	X	
04/07/2010	6.3	39.70	142.37	X	X		X			X		X	X	
18/07/2010	6.6	52.88	-169.85		X		X	X	X	X	X	X	X	X
23/07/2010	7.6	6.49	123.47		X		X	X			X	X		X
23/07/2010	7.3	6.72	123.41	X			X	X	X		X	X	X	X
25/07/2010	5.6	49.70	154.64				X					X	X	
28/07/2010	5.6	52.67	-169.41											
30/07/2010	6.3	52.50	159.84	X	X		X	X	X	X	X	X	X	X
04/08/2010	6.4	51.42	-178.65	X	X		X	X	X	X	X	X	X	X

12/08/2010	7.1	-1.27	-77.31		X		X				X	X	X	X
13/08/2010	6.9	12.48	141.48	X	X		X	X	X		X	X	X	X
14/08/2010	6.6	12.27	141.43	X			X				X	X	X	
27/08/2010	5.7	35.49	54.47							X				
03/09/2010	6.5	51.45	-175.87	X			X	X	X	X		X	X	X
08/09/2010	5.5	44.59	149.72						X					
17/09/2010	6.3	36.44	70.77		X		X					X		X
04/10/2010	6.3	24.27	125.15		X							X		
08/10/2010	6.4	51.37	-175.36	X			X	X			X		X	X
21/10/2010	6.7	24.69	-109.16				X					X	X	X
30/11/2010	6.8	28.36	139.15	X										
06/12/2010	5.7	40.90	142.97					X						
20/12/2010	6.7	28.41	59.18							X				
21/12/2010	7.4	26.90	143.70											
09/03/2011	7.5	38.44	142.84					X				X		X
09/03/2011	6.5	38.30	142.81											X
11/03/2011	9.0	38.30	142.37		X		X	X		X		X		X
12/03/2011	6.5	37.59	142.65							X		X		
13/03/2011	6.1	35.73	141.64		X			X		X		X		X
13/03/2011	5.8	37.35	142.40							X				
19/03/2011	5.9	39.70	142.90									X		
21/03/2011	5.8	36.50	70.93							X				
22/03/2011	6.5	37.24	144.00	X	X			X				X		X
22/03/2011	6.4	39.85	143.44		X									
22/03/2011	5.7	35.21	141.00									X		
25/03/2011	6.2	38.77	141.88	X				X						
27/03/2011	6.2	38.42	142.01	X				X		X		X		X
29/03/2011	6.1	37.40	142.01	X								X		X
30/03/2011	5.8	36.14	142.90		X							X		
07/04/2011	7.1	38.28	141.59	X	X			X				X		
07/04/2011	6.6	17.21	-94.34									X		
11/04/2011	6.6	37.00	140.40	X	X			X		X		X		X
11/04/2011	5.8	37.79	140.81					X		X				X
12/04/2011	5.9	37.11	140.37	X				X						
14/04/2011	5.8	35.56	141.88	X										
21/04/2011	5.8	40.31	143.63					X		X				X
23/04/2011	6.0	39.10	142.87	X				X		X		X		X
04/05/2011	5.5	37.04	143.25											X
05/05/2011	6.1	38.17	144.03	X	X			X		X		X		X
05/05/2011	5.8	55.02	-160.69	X	X			X		X		X		X
05/05/2011	5.7	55.09	-160.54	X				X		X		X		X
05/05/2011	5.7	16.78	-98.62									X		X
07/05/2011	5.7	40.24	142.24	X				X		X				X
13/05/2011	6.1	37.40	141.34	X								X		
14/05/2011	6.0	36.41	70.75		X			X		X		X		X
19/05/2011	5.9	39.15	29.10							X				X
23/05/2011	5.7	37.66	141.66							X				
24/05/2011	5.8	39.72	143.24											X
03/06/2011	6.2	37.29	143.91	X	X			X		X		X		X
14/06/2011	5.8	37.73	143.52											X
15/06/2011	5.7	27.78	57.77									X		

Table DR3: List of processed events, showing date, magnitude, epicentral distance, backazimuth and for which station. Data from National Earthquake Information Center Earthquake Catalog

				Used at stations						
Date (date/month/ year)	**Mag**	**Lat (°)**	**Lon (°)**	**STO**	**INC**	**ALT**	**BAS**	**BIG**	**ORE**	**HOY**
04/10/1995	**7.0**	**-2.75**	**-77.88**						**X**	
23/11/1995	**7.3**	**28.83**	**34.80**						**X**	
04/02/1996	**6.6**	**27.29**	**100.28**						**X**	
08/02/1996	**7.2**	**45.32**	**149.89**						**X**	
31/03/1996	**6.3**	**52.21**	**-168.73**						**X**	
08/05/1996	**6.2**	**43.71**	**147.61**						**X**	
03/06/1996	**7.1**	**10.80**	**-42.25**						**X**	
22/06/1996	**7.0**	**51.57**	**159.12**						**X**	
05/09/1996	**6.2**	**9.36**	**-84.27**						**X**	
10/10/1996	**6.9**	**34.56**	**32.13**						**X**	
20/11/1996	**7.1**	**35.35**	**78.13**						**X**	
11/12/1996	**7.0**	**0.87**	**-30.04**						**X**	
23/12/1996	**6.5**	**43.21**	**138.92**						**X**	
24/01/1997	**7.1**	**-22.00**	**-65.72**						**X**	
14/05/1997	**6.1**	**31.82**	**130.28**						**X**	
15/07/1997	**6.1**	**43.25**	**146.38**						**X**	
14/08/1997	**6.2**	**25.03**	**125.77**						**X**	
03/09/1997	**6.8**	**3.85**	**-75.75**						**X**	
14/10/1997	**6.7**	**36.38**	**22.07**						**X**	
16/11/1997	**6.1**	**43.81**	**145.02**						**X**	
06/12/1997	**7.8**	**54.84**	**162.04**						**X**	
21/02/1998	**6.4**	**36.48**	**71.09**						**X**	
04/05/1998	**7.9**	**22.31**	**125.31**						**X**	
31/05/1998	**7.0**	**37.11**	**70.11**						**X**	
21/08/1998	**7.1**	**28.93**	**139.33**						**X**	
13/05/1999	**6.5**	**43.03**	**143.84**						**X**	
16/06/1999	**7.0**	**18.39**	**-97.44**						**X**	
12/07/1999	**7.0**	**15.78**	**-88.33**						**X**	
21/08/1999	**6.9**	**9.04**	**-84.16**						**X**	
09/11/1999	**6.5**	**36.52**	**71.24**						**X**	
29/01/2000	**6.8**	**43.05**	**146.84**						**X**	
18/07/2000	**6.6**	**36.28**	**70.92**						**X**	
21/07/2000	**6.2**	**36.51**	**140.98**						**X**	
24/07/2001	**6.3**	**-19.55**	**-69.23**				**X**	**X**		
28/07/2001	**6.6**	**59.00**	**-155.09**		**X**	**X**	**X**	**X**		
31/07/2001	**5.8**	**51.16**	**179.39**			**X**				
02/08/2001	**6.3**	**56.22**	**163.70**		**X**	**X**	**X**	**X**		
05/08/2001	**5.9**	**12.25**	**93.39**		**X**		**X**	**X**		
13/08/2001	**6.4**	**41.05**	**142.28**		**X**	**X**	**X**	**X**		**X**
17/08/2001	**5.9**	**25.79**	**126.23**		**X**		**X**	**X**		
25/08/2001	**6.0**	**7.60**	**-82.76**		**X**		**X**	**X**		
28/08/2001	**5.9**	**-21.72**	**-70.11**				**X**	**X**		
08/10/2001	**6.3**	**52.68**	**160.13**			**X**				
08/10/2001	**6.4**	**52.57**	**160.20**							**X**
09/10/2001	**5.9**	**47.74**	**155.04**				**X**	**X**		**X**
09/11/2001	**6.0**	**9.71**	**-82.25**				**X**	**X**		
14/11/2001	**7.8**	**35.88**	**90.58**		**X**					
23/11/2001	**6.0**	**36.37**	**71.44**		**X**					
18/12/2001	**6.8**	**23.99**	**122.78**		**X**					
08/12/2001	**6.2**	**28.28**	**129.46**		**X**					
03/02/2002	**6.5**	**38.61**	**31.08**		**X**					
03/02/2002	**6.5**	**38.52**	**31.22**		**X**					
02/03/2003	**5.8**	**37.68**	**141.72**				**X**	**X**		
03/03/2002	**7.3**	**36.42**	**70.46**		**X**	**X**				**X**

14/03/2002	5.9	51.55	-173.16		X					
31/03/2002	7.1	24.30	122.14		X					
22/06/2002	6.5	35.59	49.02		X					
22/06/2002	6.5	35.82	48.97		X					
31/07/2002	6.5	7.93	-82.78		X	X	X	X		
07/08/2002	5.9	7.80	-82.86				X	X		
08/08/2002	5.9	49.80	-77.82							X
20/08/2002	6.0	30.99	142.00		X		X	X		X
24/08/2002	6.1	43.16	146.08		X	X				
13/09/2002	6.5	13.02	93.09		X	X	X	X		X
03/10/2002	6.5	23.28	-108.57				X	X		
14/10/2002	6.1	41.23	142.20			X				
16/10/2002	6.2	51.91	157.22				X	X		
19/10/2002	6.3	44.26	149.87							X
24/10/2002	6.2	-19.60	29.01			X				
02/11/2002	5.8	12.70	92.86					X		X
03/11/2002	7.2	28.20	96.09				X			
03/11/2002	7.8	63.54	-147.73	X			X	X		
03/11/2002	6.4	38.95	141.94	X			X	X		
07/11/2002	6.6	51.15	179.35	X		X				
21/11/2002	5.8	12.37	-82.22	X						
26/11/2002	6.1	51.60	-173.64	X		X				
21/01/2003	6.4	13.62	-90.85	X						
22/01/2003	7.5	18.90	-104.06	X			X	X		
19/02/2003	6.6	53.60	-164.73	X	X		X	X		
24/02/2003	6.3	38.51	77.20	X						
12/03/2003	6.3	26.65	-110.56				X	X		
15/03/2003	6.0	52.22	160.27	X	X					
17/03/2003	6.1	51.31	177.93	X			X	X		
17/03/2003	7.0	51.28	177.93	X	X		X	X		
17/04/2003	6.3	37.54	96.54	X	X					X
24/04/2003	6.0	48.77	154.92	X						
29/04/2003	5.9	43.76	147.75	X						
01/05/2003	6.3	38.97	40.45	X	X					
01/05/2003	6.3	39.00	40.52	X	X					
14/05/2003	6.6	18.31	-58.60	X	X					X
19/05/2003	6.1	17.54	-105.56	X						
26/05/2003	7.0	38.86	141.50	X	X					X
15/06/2003	6.5	51.56	176.85	X						
16/06/2003	6.8	55.46	159.93	X						X
23/06/2003	6.9	51.46	176.73	X						

Table DR4. Assumed model parameters.

Description	Symbol	Value
Freely deforming upper layer		
Viscosity	H	10^{20} Pas
Yield strength	σ_y	0.1 MPa
Shear modulus	M	1 GPa
Density	P	1 kgm^{-3}
All lithologies (except dipping 'seed')		
Angle of internal friction (Buiter et al., 2006)	φ	36° (linearly reduced to 0° as plastic strain approaches 0.5)
Cohesion (Ranalli, 1995)	C	22 MPa
Crust (all lithologies)		
Coefficient of thermal expansion (Parsons and Sclater, 1977)	α	$3.28 \cdot 10^{-5} K^{-1}$
Isobaric heat capacity	C_p	800 $Jkg^{-1}K^{-1}$
Shear modulus	μ	25 GPa
-Continental (upper and lower)		
Reference density at 273 K	ρ_0	2800 kgm^{-3}
Radiogenic heat production	H_r	1.25 μWm^{-3}
Thermal conductivity	k	2.5 $Wm^{-1}K^{-1}$
-Continental (upper)		
Activation energy (Ranalli, 1995)	E	$154\ kJmol^{-1}$
Power-law exponent (Ranalli, 1995)	n	2.3
Power-law constant (Ranalli, 1995)	A	$5.02 \cdot 10^{-18} Pa^{-n} s^{-1}$
-Continental (lower)		
Activation energy (Ranalli, 1995)	E	$238\ kJmol^{-1}$
Power-law constant (Ranalli, 1995)	A	$2.08 \cdot 10^{-23} Pa^{-n} s^{-1}$
-Sediments		
Reference density at 273 K	ρ_0	2300 kgm^{-3}
Radiogenic heat production	H_r	1.0 μWm^{-3}
Activation energy (Ranalli, 1995)	E	154 $kJmol^{-1}$
Power-law exponent (Ranalli, 1995)	n	2.3

Power-law constant (Ranalli, 1995)	A	$5.02\cdot10^{-18} Pa^{-n}s^{-1}$
Thermal conductivity	k	$2.0\ Wm^{-1}K^{-1}$
Mantle		
Reference density at 273 K	ρ_0	$3300\ kgm^{-3}$
Coefficient of thermal expansion (Gillet et al., 1991)	α	$2.77\cdot10^{-5}K^{-1}+0.97\cdot10^{-8}K^{-2}T+0.32\ KT^{-2}$
Thermal conductivity (McKenzie et al., 2005)	k	$4.08\ Wm^{-1}K^{-1}(298K/T)^{0.406}$
Isobaric heat capacity (Berman and Brown, 1986)	C_p	$[1.69\cdot10^{-3}-1.42\cdot10^{4}(T/K)^{0.5}-8.27\cdot10^{8}(T/K)^{-3}]\ Jkg^{-1}K^{-1}$
Shear modulus (Karato and Wu, 1993)	μ	$80\ GPa$
-Dislocation creep		
Activation energy (Karato and Wu, 1993)	E	$540\ kJmol^{-1}$
Power-law exponent (Karato and Wu, 1993)	n	3.5
Power-law constant (Karato and Wu, 1993)	A	$2.41\cdot10^{-16} Pa^{-n}s^{-1}$
Activation volume (Karato and Wu, 1993)	V	$15\ cm^{3}mol^{-1}$
-Diffusion creep		
Activation energy (Karato and Wu, 1993)	E	$300\ kJmol^{-1}$
Power-law exponent (Karato and Wu, 1993)	n	1
Power-law constant (Karato and Wu, 1993)	A	$3.97\cdot10^{-11} Pa^{-1}s^{-1}$
Activation volume (Karato and Wu, 1993)	V	$6\ cm^{3}mol^{-1}$

Numerical modelling technique

The code is based on the marker-in-cell technique described in Gerya (2010) and represents simultaneous viscous, elastic and plastic (brittle) deformation under the assumption of conservation of energy, momentum and mass in 2 dimensions (i=1,2):

$$\frac{\partial}{\partial x_i}\left(-k\frac{\partial T}{\partial x_i}\right) = -c\rho\frac{DT}{Dt} + H_r + H_A + H_S \tag{1}$$

$$\frac{\partial \sigma'_{ij}}{\partial x_j} + \rho g_i - \frac{\partial P}{\partial x_i} = 0 \tag{2}$$

$$\frac{\partial v_j}{\partial x_j} = 0 \tag{3}$$

Where σ'_{ij} is the deviatoric stress tensor, v_j is the velocity field vector, $P = -\frac{1}{2}\sigma_{kk}$ is pressure and $H_r + H_A + H_S$ is the total rate of energy change due to radiogenic, adiabatic and shear heating respectively. $\frac{DT}{Dt}$ is the material time derivative of temperature. The adiabatic heat production is approximated(Gerya and Yuen, 2003) as $H_a \approx T\alpha v_z g$.

Strain rate is related to the velocity field by $\dot{\varepsilon}_{ij} = \frac{1}{2}\left(\frac{\partial v_i}{\partial x_j} + \frac{\partial v_j}{\partial x_i}\right)$ and is assumed to be the mutual contribution from brittle, elastic and viscous deformation:

$$\dot{\varepsilon}'_{ij} = \dot{\varepsilon}'_{ij(elastic)} + \dot{\varepsilon}'_{ij(plastic)} + \dot{\varepsilon}'_{ij(viscous)} = +\frac{1}{2\mu}\frac{D\sigma'_{ij}}{Dt} + \chi\frac{\sigma'_{ij}}{2\sigma_{II}} + \frac{1}{2\eta_{(viscous)}}\sigma'_{ij} \tag{4}$$

Where the plastic multiplier, χ is nonzero only if $\sigma_{II} = \sigma_{yield}$ which is the Mohr-Coulomb failure limit:

$$\sigma_{yield} = C + P\sin(\varphi) \tag{5}$$

The brittle strength is taken to decrease with increasing brittle strain though a linear reduction of the friction angle (Buiter et al., 2006) until a value of 0 is reached at a strain of 0.1. It is this strain weakening that allows for a localized interface between the upper and lower plates of a subduction zone. The viscous rheology depends on composition, temperature, pressure and stress:

$$\eta = \frac{1}{2A\sigma_{II}^{n-1}} \exp\left(\frac{E+PV}{RT}\right) \tag{6}$$

For the mantle, the simultaneous effect of dislocation and diffusion creep (Karato and Wu, 1993) is considered:

$$\dot{\varepsilon}'_{ij(viscouos)} = \dot{\varepsilon}'_{ij(dislocation)} + \dot{\varepsilon}'_{ij(diffusion)} = \frac{1}{2\eta_{dislocation}}\sigma'_{ij} + \frac{1}{2\eta_{diffusion}}\sigma'_{ij} = \frac{1}{2}\left(\frac{1}{\eta_{dislocation}} + \frac{1}{\eta_{diffusion}}\right)\sigma'_{ij} \tag{7}$$

Thus, the effective viscosity is given by:

$$\eta_{eff} = \left(\frac{1}{\eta_{dislocation}} + \frac{1}{\eta_{diffusion}}\right)^{-1} \tag{8}$$

Densities are temperature-dependent, and for the mantle we employ a temperature-dependent coefficient of thermal expansion (Gillet et al., 1991). For remaining lithologies we assume a constant (with temperature) coefficient of expansion (McKenzie et al., 2005). Following the Boussinesq approximation (Ranalli, 1995), density changes due to temperature changes are assumed to affect only the momentum equation (2), but are ignored in the continuity equation (3).

For definitions of the remaining terms we refer to earlier works using similar nomenclature and methods (Gerya and Yuen, 2007; Petersen et al., 2010) and Table S1.

A stress-free surface is represented by employing a “sticky-air” approach (Crameri et al., 2012) by letting the initial upper 40 km of the modelling domain have little mass and low (relative to the time scale of thermal evolution of the lithosphere) viscosity of 10^{20} *Pa s*. Furthermore, we ensure that negligible surface stresses form by also setting a plastic yield limit of 0.1 *MPa* (similar to the numerical precision of the modelling method) for the “air” layer (Petersen et al., 2015). This renders the surface effectively stress-free, even during rapid surface movements, and dynamically limits the effective viscosity only when needed (a beneficial property for especially iterative thermo-mechanical solution strategies).

Surface processes are represented as a simple diffusion process with a diffusivity of $6.6 \cdot 10^{-6} m^2/s$ (Kooi and Beaumont, 1994). Practically, erosion and sedimentation are implemented by converting markers to air or sediment, respectively (Gerya and Yuen, 2003). Experiments not presented here indicate that the employment of such surface processes does not appear to affect the general results outlined in this paper.

The model domain is initially 2000 km wide and 600 km deep. Compression and extension is applied by moving the right boundary of the modelling domain. Initial crustal thickness is 35 km and the thermal lithosphere is 150 km. The thermal lithosphere is here defined as a conductively steady-state layer above an isentropic asthenosphere that initially has a constant potential temperature of 1315 °C. Initial deformation is seeded by a weak, dipping (30°) and thin (2 km) layer within the mantle lithosphere where the friction angle is 0°.

References:

Buiter, S.J.H., Babeyko, A.Y., Ellis, S., Gerya, T.V., Kaus, B.J.P., Kellner, A., Schreurs, G., and Yamada, Y., 2006, The numerical sandbox: comparison of model results for a shortening and an extension experiment: Geological Society, London, Special Publications, v. 253, no. 1, p. 29–64, doi: 10.1144/GSL.SP.2006.253.01.02.

Crameri, F., Schmeling, H., Golabek, G.J., Duretz, T., Orendt, R., Buiter, S.J.H., May, D.A., Kaus, B.J.P., Gerya, T.V., and Tackley, P.J., 2012, A comparison of numerical surface topography calculations in geodynamic modelling: an evaluation of the "sticky air" method: Geophysical Journal International, v. 189, no. 1, p. 38–54, doi: 10.1111/j.1365-246X.2012.05388.x.

Gerya, T., 2010, Introduction to Numerical Geodynamic Modelling: Cambridge University Press, Cambridge, UK ; New York.

Gerya, T.V., and Yuen, D.A., 2003, Characteristics-based marker-in-cell method with conservative finite-differences schemes for modeling geological flows with strongly variable transport properties: Physics of the Earth and Planetary Interiors, v. 140, no. 4, p. 293–318, doi: 10.1016/j.pepi.2003.09.006.

Gerya, T.V., and Yuen, D.A., 2007, Robust characteristics method for modelling multiphase visco-elasto-plastic thermo-mechanical problems: Physics of the Earth and Planetary Interiors, v. 163, no. 1–4, p. 83–105, doi: 10.1016/j.pepi.2007.04.015.

Gillet, P., Richet, P., Guyot, F., and Fiquet, G., 1991, High-temperature thermodynamic properties of forsterite: Journal of Geophysical Research: Solid Earth, v. 96, no. B7, p. 11805–11816, doi: 10.1029/91JB00680.

Karato, S., and Wu, P., 1993, Rheology of the Upper Mantle: A Synthesis: Science, v. 260, no. 5109, p. 771–778, doi: 10.1126/science.260.5109.771.

Kooi, H., and Beaumont, C., 1994, Escarpment evolution on high-elevation rifted margins: Insights derived from a surface processes model that combines diffusion, advection, and reaction: Journal of Geophysical Research: Solid Earth, v. 99, no. B6, p. 12191–12209, doi: 10.1029/94JB00047.

McKenzie, D., Jackson, J., and Priestley, K., 2005, Thermal structure of oceanic and continental lithosphere: Earth and Planetary Science Letters, v. 233, no. 3–4, p. 337–349, doi: 10.1016/j.epsl.2005.02.005.

Petersen, K.D., Armitage, J.J., Nielsen, S.B., and Thybo, H., 2015, Mantle temperature as a control on the time scale of thermal evolution of extensional basins: Earth and Planetary Science Letters, v. 409, p. 61–70, doi: 10.1016/j.epsl.2014.10.043.

Petersen, K.D., Nielsen, S.B., Clausen, O.R., Stephenson, R., and Gerya, T., 2010, Small-Scale Mantle Convection Produces Stratigraphic Sequences in Sedimentary Basins: Science, v. 329, no. 5993, p. 827–830, doi: 10.1126/science.1190115.

Ranalli, G., 1995, Rheology of the Earth: Springer Science & Business Media.

Figure DR1

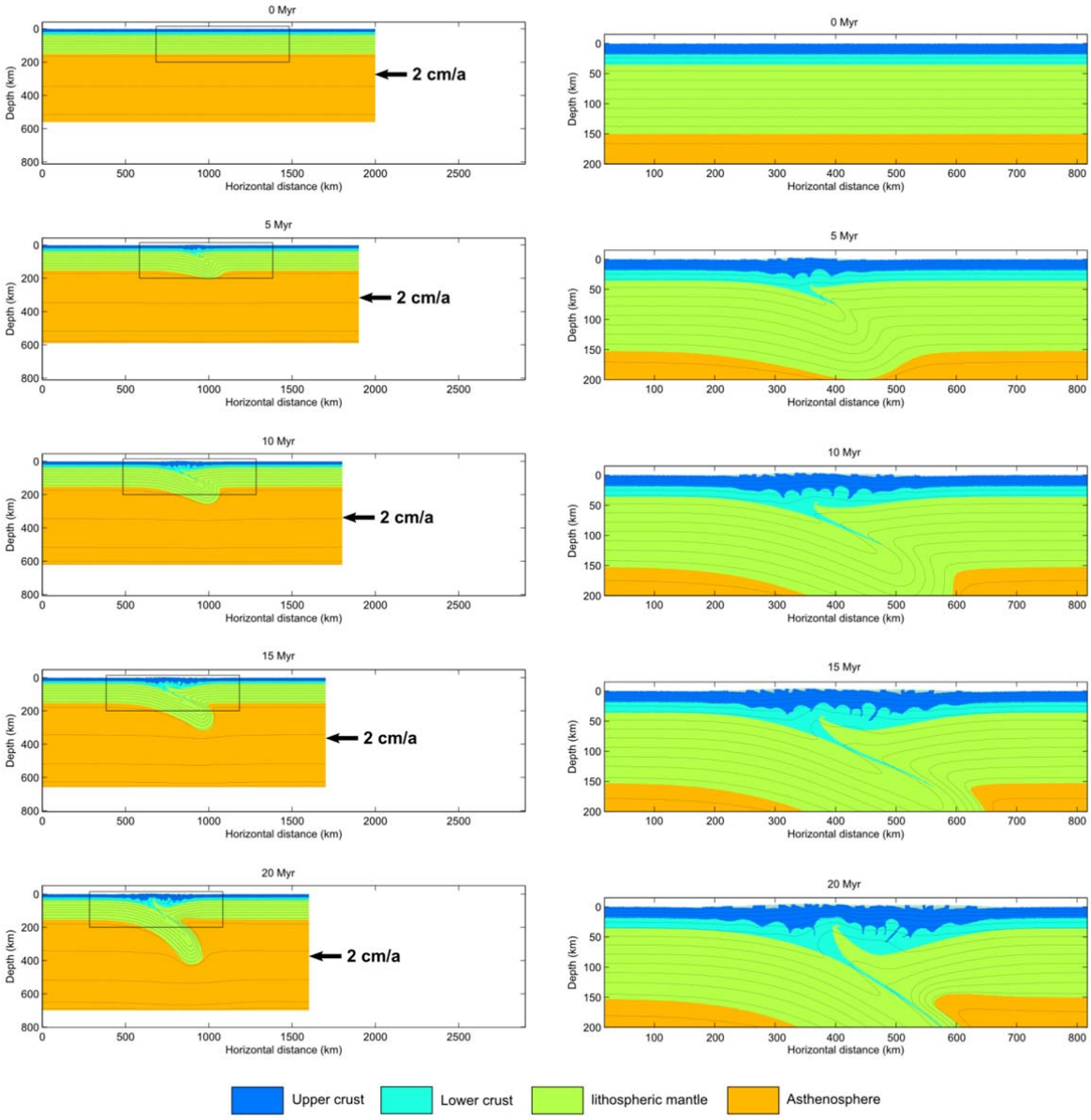

Numerical modelling results of continent-continent convergence over a period of 20 Myr and a convergence rate of 2 cm/yr. Left – whole model domain. Right – zoom into the black box shown on the left side. Dark blue – upper crust. Light blue – lower crust. Green – mantle lithosphere. Orange – Asthenosphere. An orogen is forming while the lower crust of the underthrusting continent is partially "subducted" into the lithosphere.

Figure DR2

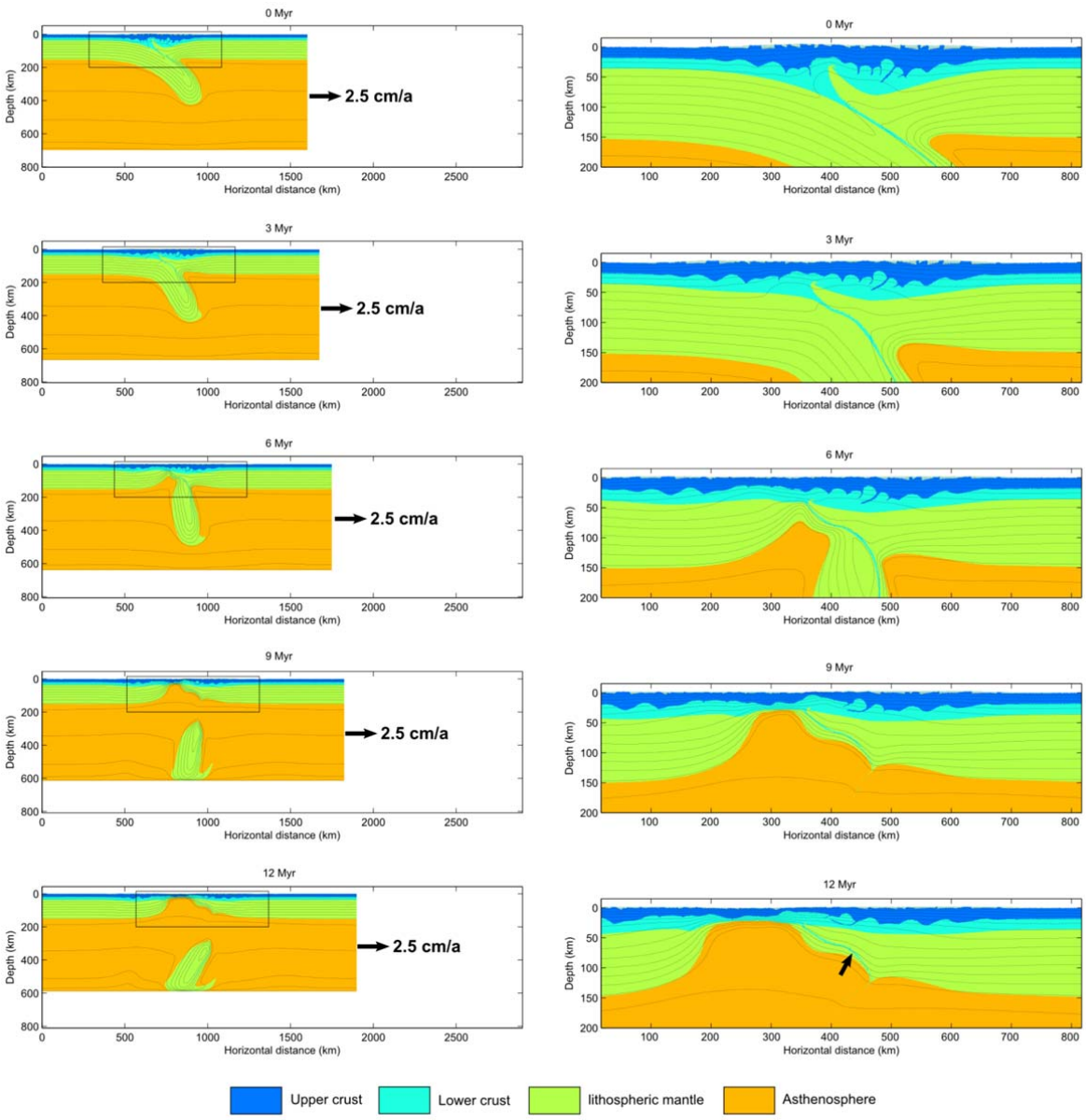

Numerical modelling results of fast extension (2.5 cm/yr) of the modelled orogen shown in Fig.DR7 over a period of 12 Myr. Colours are as in Fig. DR7. The lithosphere is delaminating after ~6 Myr, whereas the upper part of the subducted lower crust remains at place within the lithospheric mantle and is preserved on the right margin as a remnant orogenic structure dipping away from the rift – a template for the FR structure.

Figure DR3

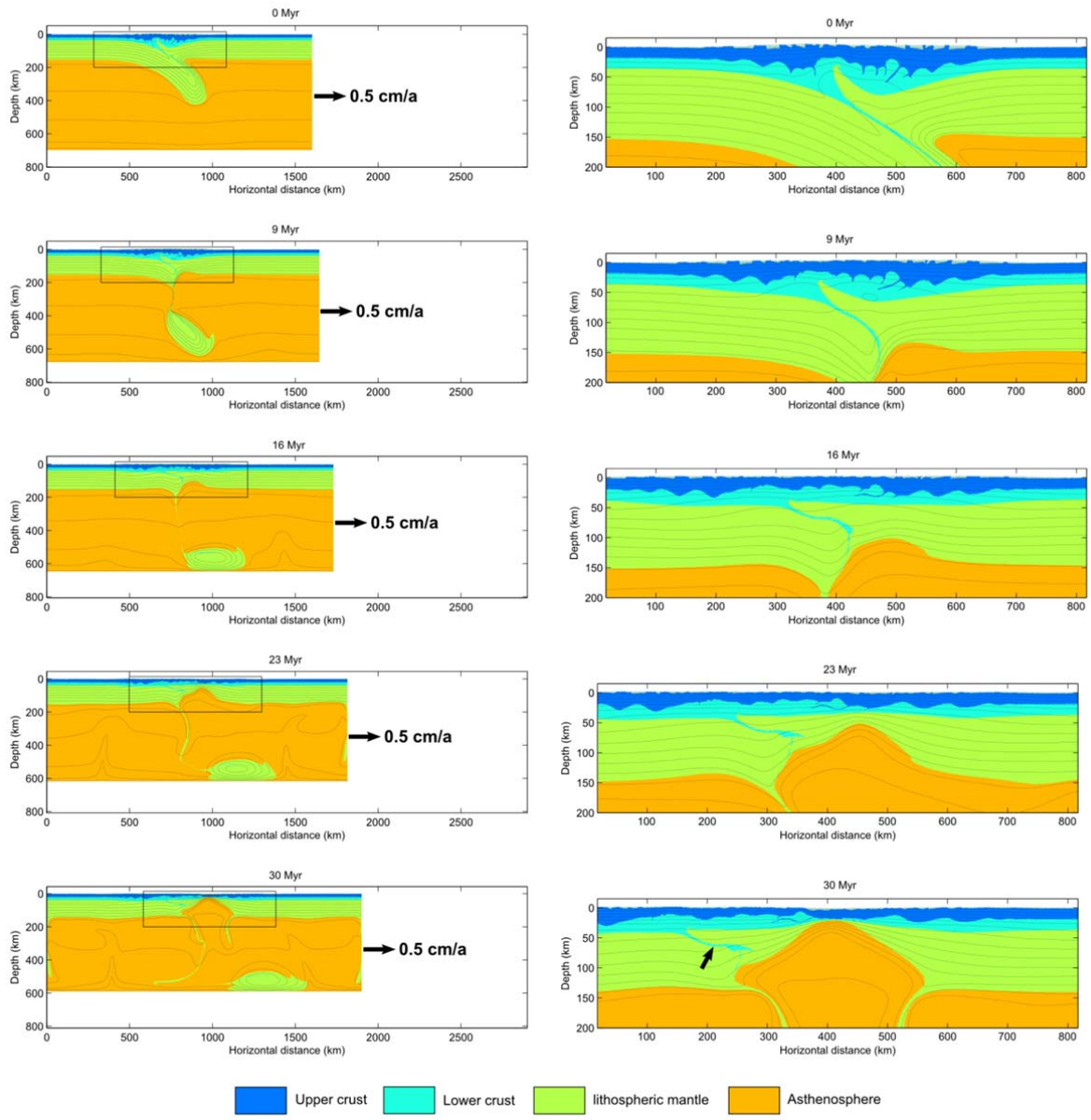

Numerical modelling results of slow extension (0.5 cm/yr) of the modelled orogen shown in Fig.DR7 over a period of 60 Myr. The lithosphere is delaminating within the first ~9 Myr, whereas the upper part of the subducted lower crust remains at place within the lithospheric mantle and is preserved on the left margin as a remnant orogenic structure dipping towards the rift – a template for the CF structure.